Fuel 301 (2021) 121077

Contents lists available at ScienceDirect

Fuel

journal homepage: www.elsevier.com/locate/fuel

Significant enhancement in CH_4/N_2 separation with amine-modified zeolite Y

Yaqi Wu [a,b], Danhua Yuan [a], Shu Zeng [a,b], Liping Yang [a,b], Xingzong Dong [a,b], Quan Zhang [a,b], Yunpeng Xu [a,*], Zhongmin Liu [a]

[a] Dalian National Laboratory for Clean Energy, Dalian Institute of Chemical Physics, Chinese Academy of Sciences, Dalian 116023, China
[b] University of Chinese Academy of Sciences, Beijing 100049, China

ARTICLE INFO

Keywords:
CH_4/N_2 separation
Amine modification
Zeolite Y
Natural gas purification
Adsorption separation

ABSTRACT

Adsorption based process for CH_4/N_2 separation is promising and attractive while it remains a challenge endeavor due to the lack of efficient adsorbents. In this work, amine ion-exchanged Y zeolites were developed for CH_4/N_2 separation. By simple ion-exchanged with tetramethylammonium cation (TMA^+) and choline cation (Ch^+), CH_4 adsorption amounts of the resulting adsorbents were obviously increased while their N_2 adsorption amounts were significantly decreased. Consequently, CH_4/N_2 separation performances of resulted samples were greatly improved compared to pristine NaY. CH_4/N_2 selectivities of resulting sample TMAY and ChY were up to 6.32 and 6.50, respectively, at 25 °C and 100 kPa. Monte Carlo calculations were used to study the interaction affinity for CH_4 and N_2 on the adsorbents. Breakthrough experiments were further confirmed the excellent separation performances of TMAY and ChY. The excellent separation performances of the resulting adsorbents verified the efficiency of the simple ion-exchange strategy and the application potential of the adsorbents.

1. Introduction

Natural gas continues to gain extensive attention as it takes an increasing proportion in the worldwide energy structure. However, in large amount of natural gas reserves, such as shale gas, coal mine methane, CH_4 is generally mixed a considerable portion of N_2 [1,2]. Moreover, natural gases that contain significant amounts of nitrogen need to be upgraded in order to meet the pipeline quality for minimum heating value specifications, typically >90% methane [3]. The similar properties of N_2 and CH_4 makes the removal of N_2 from CH_4 to be quite difficult. CH_4/N_2 separation is one of the most challenging endeavor in gas separation. Currently, the separation of N_2 from CH_4 is accomplished mainly by cryogenic distillation which is highly energy-consuming and expensive [4]. Alternative technologies to cryogenic distillation process rely on the development of selective adsorbents that could provide substantial energy savings. However, it remains to be particularly difficult as satisfactory adsorbents are still lacking. Relevant works in these areas mostly focused on porous materials including zeolites [5–8], porous carbonaceous materials [9–11], metal organic frameworks (MOFs) [12–14] and porous organic polymers [15].

Zeolites are very traditional porous materials with low cost, high stability and mature industrialized synthesis technology, which should be one of the most promising adsorbents for CH_4/N_2 separation. Nevertheless, due to the strong polarity and strong electrostatic field in their cavities, zeolites often exhibited high adsorption capacity towards CH_4 with high polarizability as well as N_2 with high quadrupole moment [16]. Therefore, the selectivity of traditional zeolites towards CH_4/N_2 were always not high [6,8,17–19]. How to increase the separation performance of zeolites has always been a challenging endeavor. If the CH_4/N_2 selectivity of traditional zeolites can be greatly improved only by some simple modifications, it would be of great significance for zeolites to be applicable CH_4/N_2 adsorbents. In our recent work, the strategy of decorating zeolites with MOFs subunits proved to be efficient for the separation of CH_4/N_2 [20].

In the present work, a series of CH_4/N_2 separation adsorbents were developed by amine ion-exchange with zeolite NaY. Tetramethylammonium chloride (TMAC), choline chloride (ChCl) and tetraethylammonium chloride (TEAC) were used to decorate the zeolite pores. With the introduction of amine cations, CH_4/N_2 selectivities of zeolite Y were greatly improved. Molecular simulation and isosteric heats of adsorption were used to investigate the interactions of adsorbents and adsorbates. Additionally, breakthrough experiments were performed

* Corresponding author.
E-mail address: xuyunpeng@dicp.ac.cn (Y. Xu).

https://doi.org/10.1016/j.fuel.2021.121077
Received 30 March 2021; Received in revised form 10 May 2021; Accepted 15 May 2021
Available online 24 May 2021

with binary CH_4/N_2 mixtures to further investigate the dynamic separation performances of the resulting adsorbents.

2. Experimental section

2.1. Materials

Zeolite NaY ($SiO_2/Al_2O_3 = 5.4$) was purchased from DALIAN HAXIN CHEMICAL INDUSTRIAL CO., LTD. Tetramethylammonium chloride (TMAC, AR, 98%), tetraethylammonium chloride (TEAC, AR, 98%) and Choline Chloride (ChCl, >98%) were purchased from Aladdin and used without further treatment.

2.2. Preparation of the adsorbent

TMAY and TEAY. 5 g of Zeolite NaY in 250 mL of 1 M TMAC (or 1 M TEAC) solution was refluxed at 80 °C under stirring for 4 h, respectively, followed by filtration and washing with deionized water 3 times. The above ion exchanged procedure was repeated three times. The samples were dried in an oven at 120 °C for 12 h.

ChY. 5 g of Zeolite NaY in 250 mL of 1 M ChCl solution was refluxed at 80 °C under stirring for 4 h, respectively, followed by filtration and washing with deionized water 3 times. The above ion exchanged procedure was repeated three times. The samples were dried in an oven at 120 °C for 12 h.

2.3. Characterizations

The powder X-ray diffraction (XRD) measurements were carried out on a PANalytical X'Pert PRO X-ray diffractometer with Cu-Kα radiation (λ = 1.54059 Å), operating at 40 kV and 40 mA. The Na content of the samples was determined by X-ray fluorescence (XRF, PANalytical Axios advanced). The morphologies of the adsorbents were measured on Hitachi SU8020 cold field emission scanning electron microscope (SEM). Thermogravimetric analysis (TGA) were performed on an SDT Q600 (TA Instruments-Waters LLC, USA) under nitrogen atmosphere (flow rate 100 mL/min). Fourier transform infrared spectroscopy (FTIR) spectra were carried out using a Bruker Vertex-70 spectrophotometer. N_2 adsorption–desorption isotherms, specific surface areas and porosity of samples were measured by Micromeritics, ASAP 2020, USA under liquid nitrogen bath (-196 °C). The Brunauer-Emmett-Teller surface area (S_{BET}), total pore volume (V_t) and micropore surface area (S_{micro}) of resulting adsorbents were calculated based on the Brunauere-Emmette-Teller (BET) equation and t-plot method, respectively. The N and C content of resulting adsorbents were measured by an elemental analyzer (Elementar; Model: vario EL cube; Germany). All the solid-state nuclear magnetic resonance (NMR) experiments were performed on a Bruker Avance III 600 spectrometer equipped with a 14.1 T wide-bore magnet. The resonance frequencies for ^{13}C and ^{23}Na were 150.9 MHz and 158.7 MHz, respectively. The ^1H–^{13}C cross-polarization/magic-angle spinning (CP/MAS) was carried out using a 4 mm WVT probe, with spinning rate of 12 kHz. A recycle delay of 2 s and a contact time of 3 ms was used. Chemical shifts were referenced to adamantane with the upfield methene peak at 29.5 ppm for ^{13}C CP spectra. The ^{23}Na MAS spectra were recorded using a 3.2 mm probe with spinning rate of 22 kHz. A ^{23}Na rf field of 0.833 MHz and a recycle delay of 1 s were set to the sequence. Chemical shifts were referenced to 1.0 M NaCl solution at 0 ppm.

2.4. Gas adsorption

Single component adsorption isotherms of CH_4 and N_2 on NaY, TMAY, ChY and TEAY were measured on a Micromeritics Gemini VII 2390 adsorption apparatus under 25 °C in the pressure range of 0–103 kPa. The CH_4 and N_2 with high purity of 99.999% were used without any purification.

2.5. Breakthrough experiments

Breakthrough experiments were performed on a self-assembly experimental setup as we reported earlier [20]. Breakthrough experiments were carried out with binary mixtures of equimolar CH_4/N_2 (50/50, v/v). An 8 mm diameter and 30 cm long stainless steel adsorption column was packed with 6 g of sample pellets. Breakthrough experiments were performed at 25 °C for feed gas at 100 kPa flowing at 10 mL/min.

2.6. Adsorption selectivity

Dual-site Langmuir-Freundlich (DSLF) model was combined with ideal adsorption solution theory (IAST) to calculate the CH_4/N_2 adsorption selectivity [21,22]. Firstly, CH_4 and N_2 single component adsorption isotherms were fitted by DSLF model, which can be expressed as follows:

$$q = q_1 b_1 p^{1/n_1}/\left(1 + b_1 p^{1/n_1}\right) + q_2 b_2 p^{1/n_2}/\left(1 + b_2 p^{1/n_2}\right) \quad (1)$$

where q is the amounts adsorbed of an adsorbent in equilibrium (mmol/g), q_1 and q_2 are the saturation uptakes of site 1 and 2 (mmol/g), b_1 and b_2 are the affinity coefficients for sites 1 and 2 (kPa^{-1}), p is the pressure (kPa) of the bulk gas at equilibrium with the adsorbed phase, n_1 and n_2 represent the deviations from an ideal homogeneous surface for sites 1 and 2 (dimensionless), respectively.

Secondly, the final adsorption selectivity of adsorbate 1 to adsorbate 2 was calculated as follows:

$$S_{1/2} = \frac{x_1/y_1}{x_2/y_2} \quad (2)$$

where x_1 and x_2 are the mole fractions of components 1 and 2 in the adsorbed phase, respectively, and y_1 and y_2 are the mole fractions of components 1 and 2 in the gas phase, respectively.

2.7. Isosteric heats of adsorption

The isosteric heats of adsorption were calculated with a built-in heats of adsorption function in Micromeritics Gemini VII 2390 analyzer, which is based on the Clausius-Clapeyron equation [23]:

$$\frac{\Delta Hs}{RT^2} = -\left(\frac{\partial lnP}{\partial T}\right)_q \quad (3)$$

where ΔH_s is the isosteric heat of adsorption (kJ/mol), P is the pressure described in kPa, q is the adsorbed amount in mmol/g, R is the universal gas constant, T is the temperature in K.

2.8. Molecular simulation details

Energy distribution of CH_4 and N_2 in adsorbents were calculated using the Sorption module in Materials Studio according to the reported studies [21]. Si(1)Al(1) cluster was adopted as zeolite framework model [24,25]. The van der Waals interactions were described by Universal Force Field [26] and the partial atomic charges were calculated by the QEq algorithm. The Si(1)Al(1) cluster, cations and adsorbate molecules were geometry-optimized before simulation. The cluster and cations were kept rigid during the simulation. During calculation, one molecule of CH_4 and N_2 were loaded into the framework model through Metropolis Monte Carlo method [27].

3. Results and discussion

3.1. Characterization of adsorbents

Fig. 1 shows the XRD patterns of pristine NaY, TMAY, ChY and TEAY.

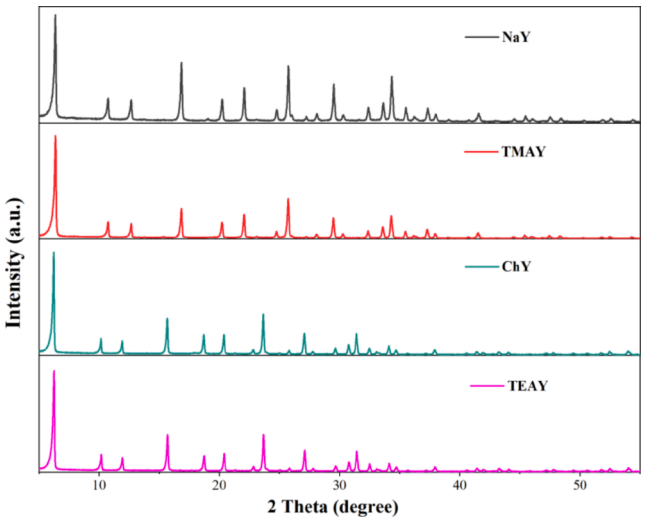

Fig. 1. XRD patterns of NaY, TMAY, ChY and TEAY.

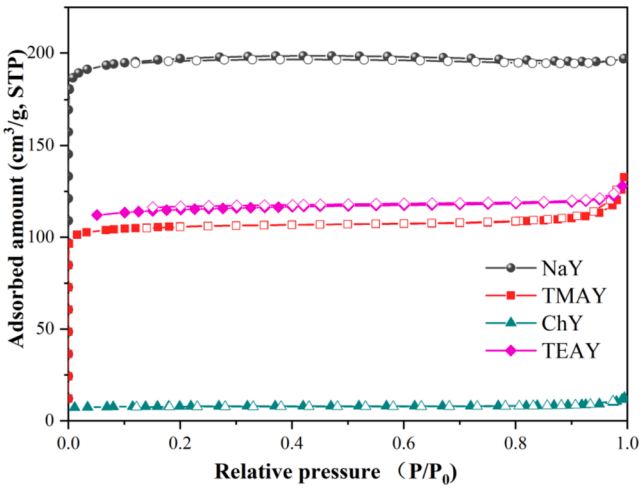

Fig. 3. N_2 adsorption–desorption isotherms of NaY, TMAY, ChY and TEAY, open symbols: adsorption, solid symbols: desorption.

Crystalline structure of zeolite Y remain unchanged as the XRD peaks of TMAY, ChY and TEAY agree well with the pristine NaY. The SEM images of the adsorbents were presented in Fig. 2, which compared to NaY, no obvious morphology changes of the TMAY, ChY and TEAY were observed. XRD and SEM results suggested that the ion-exchange with TMAC, ChCl and TEAC was mild.

Fig. 3 shows the N_2 adsorption–desorption isotherms of NaY, TMAY, ChY and TEAY. The isotherms of pristine NaY, TMAY, ChY and TEAY all typically exhibited type-I isotherms, indicating the microporous properties of the adsorbents. With the decoration of tetramethylammonium cation (TMA^+), choline cation (Ch^+) and tetraethylammonium cation (TEA^+), the equilibrium N_2 adsorbed amount of Y zeolite decreased to a large extent. Table 1 listed the textural parameters and element analysis results of NaY, TMAY, ChY and TEAY. The results indicated that ion-exchange with TMA^+, Ch^+ and TEA^+, lead to dramatical decreases in S_{BET} and S_{micro} of Y zeolite, which compared to NaY (S_{BET} of 654 m^2/g and S_{micro} of 609 m^2/g), S_{BET} and S_{micro} of TMAY decreased to 353 m^2/g and 327 m^2/g, respectively. The difference between the TMA^+ and Ch^+ is that one of the four $–CH_3$ groups in TMA^+ is replaced by a longer and larger $–CH_2CH_2OH$ group, resulting in the occupation of more porosity of zeolite. Therefore, S_{BET} and S_{micro} of ChY sharply decreased to 26 $m^2/$

Table 1
Textural and chemical properties of NaY, TMAY, TEAY and ChY.

Sample	S_{BET} m^2/g	S_{micro} m^2/g	V_{micro} cm^3/g	Na wt %[a]	N wt %[b]	C wt %[b]
NaY	654	609	0.3	9.89	–	–
TMAY	353	327	0.18	6.19	1.56	5.38
TEAY	365	336	0.19	7.78	0.84	5.21
ChY	26	22	0.01	6.36	1.46	6.04

[a] Na content were measured by XRF. [b]N and C content were measured by elemental analyser.

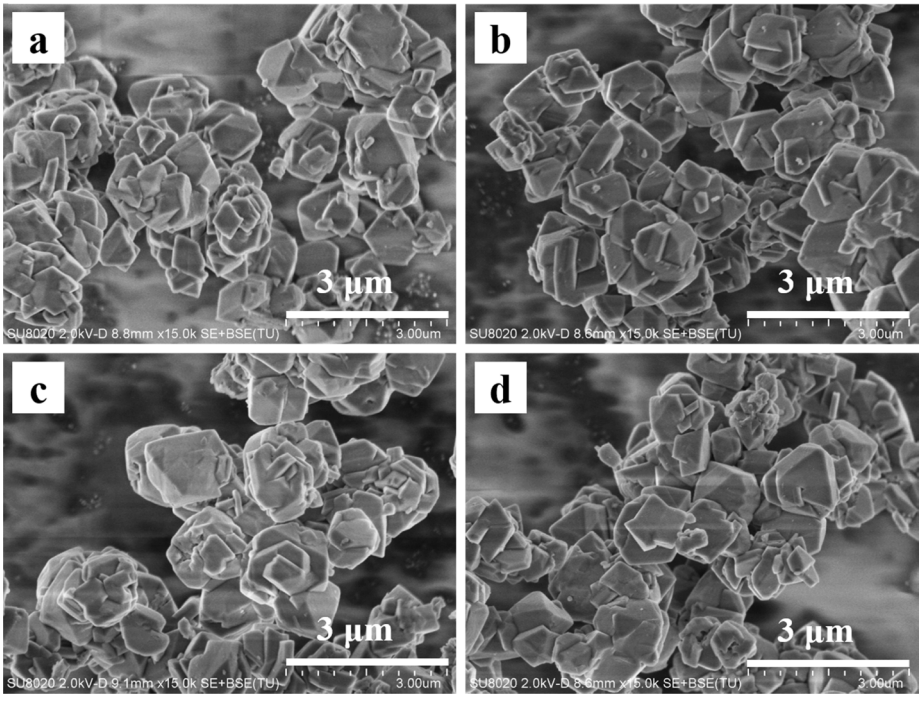

Fig. 2. SEM images of (a) NaY, (b) TMAY, (c) ChY and (d) TEAY.

g and 23 m^2/g, respectively. Elemental analysis results also demonstrated that partial of the Na^+ were exchanged by the TMA^+, Ch^+ and TEA^+. N and C content also confirmed the successful modification of TMA^+ and Ch^+ inside zeolite pores. Due to larger $–CH_2CH_3$ groups of TEA^+, relatively less TEA^+ were exchanged into the zeolite pores.

Fig. 4 shows the TGA curves of NaY, TMAY and ChY. Only one weight loss steps below 200 °C was observed for NaY, which could be ascribed to the removal of guest molecules (mainly water) adsorbed on the surfaces. Besides the water weight loss peak before 200 °C, a weight loss step in the range of 450–500 °C appeared for TMAY and two obvious weight loss steps in the range of 300–350 °C and 400–450 °C occurred for ChY, which could be attributed to the decomposition of the organic TMA^+ and Ch^+. Fig. 5 presents the FTIR spectra of the pristine NaY, TMAY and ChY. It was clearly shown that compared with NaY, an absorption band at 3018 cm^{-1} assigned to N–H stretching vibrations and a strong band at 1490 cm^{-1} assigned to the asymmetric methyl deformation vibrations were observed for TMAY [28,29]. For ChY, a band at 1490 cm^{-1} assigned to the asymmetric methyl deformation vibrations was also observed.

The assignment of ^{23}Na MAS NMR spectra of NaY, TMAY and ChY are presented in Fig. 6. It is indicating that Na^+ in supercages and sodalite units were mainly exchanged by TMA^+ and Ch^+[30]. Fig. 7 shows the ^{13}C CP/MAS NMR spectra and assignment of C environment of TMAY and ChY. For sample TMAY, the peak at 56.2 ppm was typical for $–CH_3$ groups of TMA^+ [31]. Three distinct resonances were observed for ChY, which resonances at 54.8 ppm, 56.9 ppm and 70.5 ppm can be assigned to $–CH_3$ groups, $–CH_2OH$ and N-CH_2- of Ch^+, respectively. ^{23}Na MAS NMR and ^{13}C CP/MAS NMR spectra further confirmed the successful introduction of TMA^+ and Ch^+ into zeolite Y.

3.2. CH_4 and N_2 single component adsorption isotherms

Fig. 8 shows the adsorption isotherms of CH_4 and N_2 on NaY, TMAY, ChY and TEAY at 25 °C for pressures up to 103 kPa. It can be clearly seen that CH_4 adsorption amounts of all the adsorbents were higher than that of N_2 adsorption amounts over the pressure range measured, suggesting that all the adsorbents exhibited preferential adsorption of CH_4 over N_2.

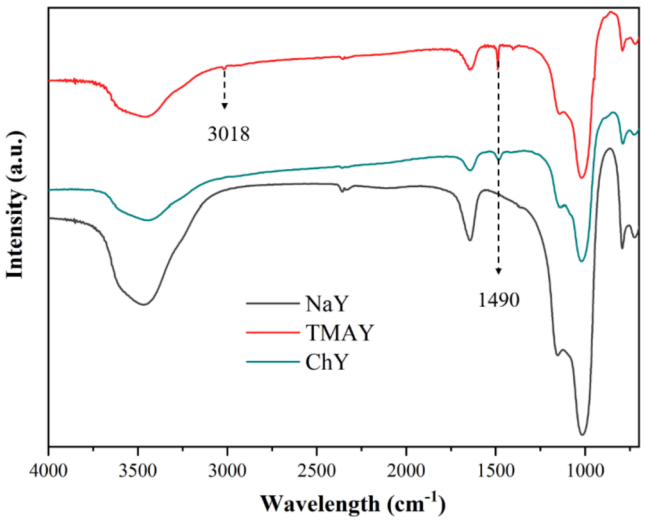

Fig. 5. FTIR spectra of NaY, TMAY and ChY.

Interestingly, after ion-exchange with TMA^+ and Ch^+, both CH_4 adsorption amount of TMAY and ChY increased significantly compared to the pristine NaY. At 25 °C and 100 kPa, CH_4 uptakes were increased from 0.39 mmol/g of NaY to 0.41 mmol/g of ChY and even 0.51 mmol/g of TMAY. On the contrary, after ion-exchange, N_2 adsorption amounts of TMAY and ChY decreased to a large extent compared to NaY. At 25 °C and 100 kPa, N_2 uptakes were reduced from 0.23 mmol/g of NaY to 0.09 mmol/g of ChY and 0.11 mmol/g of TMAY, respectively. While for TEAY, due to its lower loading of TEA^+, CH_4 and N_2 adsorption amounts were less affected by the TEA^+ and mainly influenced by the decrease of S_{BET}. Both CH_4 and N_2 adsorption amounts of TEAY decreased compared with NaY.

3.3. CH_4/N_2 adsorption selectivities

Ideal adsorbed solution theory (IAST) was used to predict the

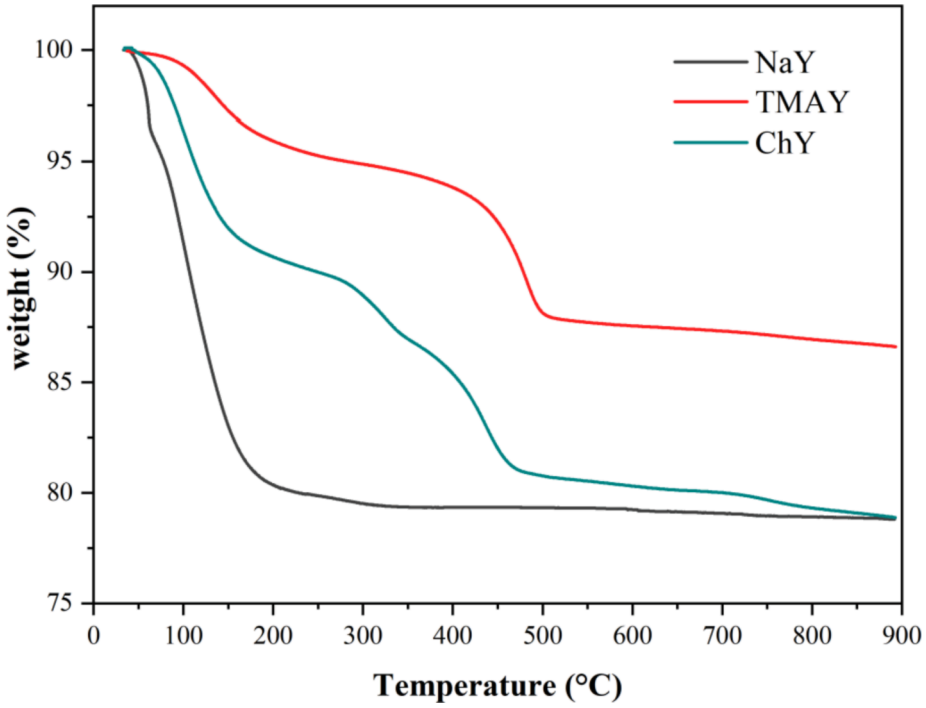

Fig. 4. TGA curves of NaY, TMAY and ChY.

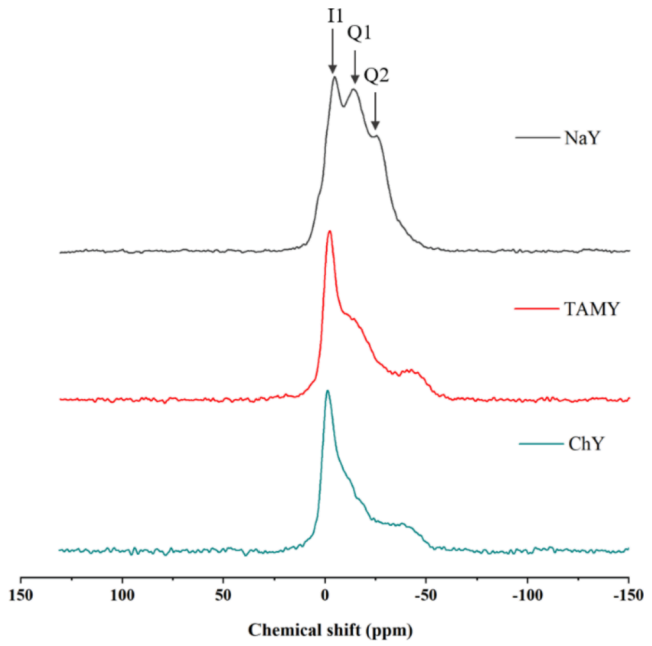

Fig. 6. ^{23}Na MAS NMR spectra of dehydrated zeolites NaY, TAMY and ChY. I1: sodium cations in the centers of hexagonal prisms, Q1: sodium cations in supercages, Q2: sodium cations in sodalite units.

adsorption selectivities for binary CH_4/N_2 mixtures on the adsorbents based on the single component adsorption isotherms. The adsorption isotherms were fitted to the DSLF model. Fitting parameters and correlation coefficients (R^2) of the DSLF model are presented in Table 2. The high values of correlation coefficients (R^2) indicated that CH_4 and N_2 isotherms were well-fitted. Fig. 9 presents the IAST predicted CH_4/N_2 selectivities for equimolar CH_4/N_2 (50:50) mixtures at 100 kPa and 25 °C of NaY, TMAY, ChY and TEAY. Due to increased CH_4 adsorption amounts and decreased N_2 adsorption amount, ChY and TAMY achieved much higher CH_4/N_2 selectivities than NaY. At 25 °C and 100 kPa, CH_4/N_2 selectivity for NaY was 1.79 whereas for ChY and TMAY, CH_4/N_2 selectivities increased to 6.50 and 6.32, respectively. As for TEAY, its CH_4/N_2 selectivities was slightly increased compared to NaY. As listed in Table 3, in comparison with the most reported adsorbents in the literature, CH_4/N_2 selectivity of TMAY and ChY were at relatively high levels, indicating the efficiency of the simple ion-exchange strategy. The adsorbents in this work shown some advantages over those reported ones, making them promising for industrial applications. Compare to expensive raw materials (metal salts and organic linkers) and organic solvent- and energy- consuming synthesis process of MOFs [32], the zeolite Y based adsorbents have the advantages of low cost, high stability and mature industrial synthesis technologies. For zeolites, many of zeolites shown low CH_4/N_2 selectivities and some modified zeolites require multiple modification steps despite their satisfactory separation performance.

3.4. Energy distribution of CH_4 and N_2

TMAY and ChY exhibited great advantages on both CH_4 adsorption amounts and CH_4/N_2 selectivities. Thus, molecular simulations were used to investigate the reason of increasing CH_4 adsorption capacity of zeolite Y after ion-exchange with TMA^+ and Ch^+. The energy distribution of CH_4 and N_2 during adsorption in Si(1)Al(1)-Na^+, Si(1)Al(1)-TMA^+ and Si(1)Al(1)–Ch^+ clusters were simulated. Fig. 10 and Fig. 11 shows the lowest energy frameworks and energy distribution of CH_4 and N_2 during adsorption in the clusters, respectively. The lowest energy frameworks of CH_4 and N_2 adsorption in Si(1)Al(1) clusters vary from the cation type (Fig. 10), indicating the different interactions between different cations and CH_4 and N_2. As shown in Fig. 11, the interaction energy of CH_4 in Si(1)Al(1)-TMA^+ and Si(1)Al(1)–Ch^+ clusters were much higher than that of Si(1)Al(1)-Na^+, suggesting the more favorable adsorption affinity of CH_4 with the Si(1)Al(1)-TMA^+ and Si(1)Al(1)–Ch^+ clusters than that of CH_4 and Si(1)Al(1)-Na^+ clusters. The simulation results were in accordance with the above CH_4 adsorption isotherms that with ion-exchange with TMA^+ and Ch^+, CH_4 adsorption amounts of TMAY and ChY increased a lot compared with NaY. While for N_2, because of the less favorable adsorption affinity of N_2, TMAY and ChY exhibited decreasing N_2 adsorption amounts restricted to the dramatically decreasing S_{BET} and S_{micro}.

3.5. Isosteric heats of CH_4 and N_2 adsorption

Isosteric heats of adsorption were calculated to evaluate the

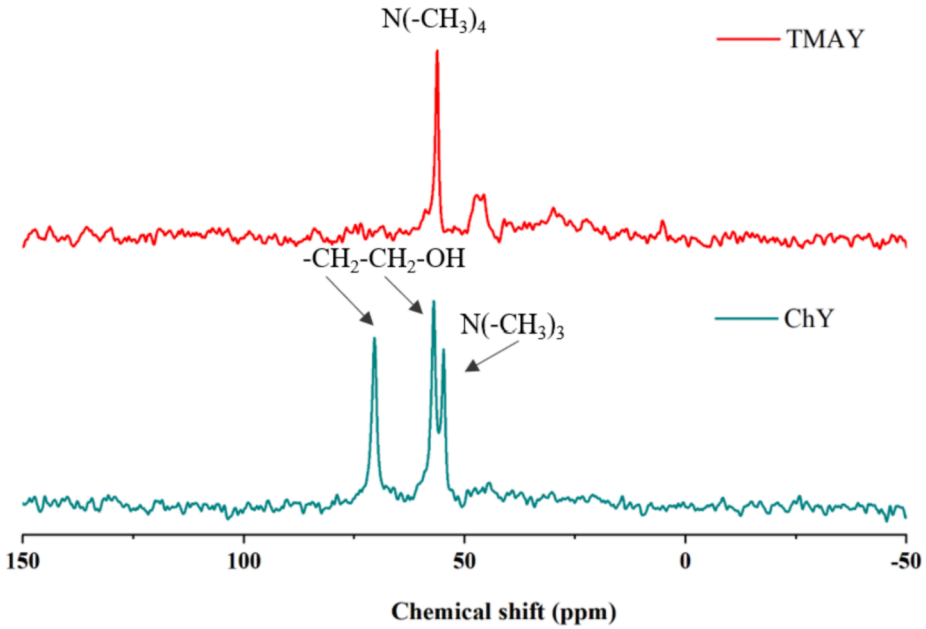

Fig. 7. ^{13}C CP/MAS NMR spectra and assignment of C environment of TMAY and ChY.

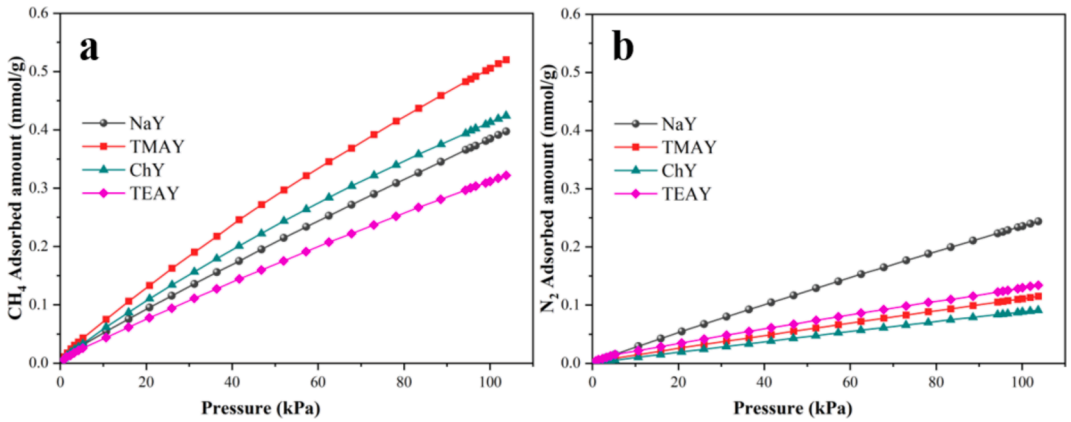

Fig. 8. (a) CH_4 and (b) N_2 adsorption isotherms of NaY, TMAY, ChY and TEAY at 25 °C, up to 103 kPa.

Table 2
Fitting parameters of DSLF model.

Parameters		q_1	b_1	n_1	q_2	b_2	n_2	R^2
NaY	CH_4	14.5475	0.0004	1.2379	0.9701	0.0008	0.8598	0.99996
	N_2	13.0649	0.0002	1.0864	0.8875	0.0009	1.0245	0.99989
TMAY	CH_4	5.9682	0.0015	1.1844	0.9566	0.0010	0.9835	0.99997
	N_2	0.9993	0.0010	1.1029	0.8782	0.0009	1.0867	0.99905
ChY	CH_4	3.0008	0.0023	1.1432	0.9565	0.0010	1.0429	0.99998
	N_2	0.8614	0.0008	1.0928	0.8362	0.0008	1.1040	0.99875
TEAY	CH_4	8.3591	0.0008	1.5232	0.9680	0.0008	0.8055	0.99999
	N_2	5.4851	0.0003	1.2293	0.9142	0.0009	1.1031	0.99986

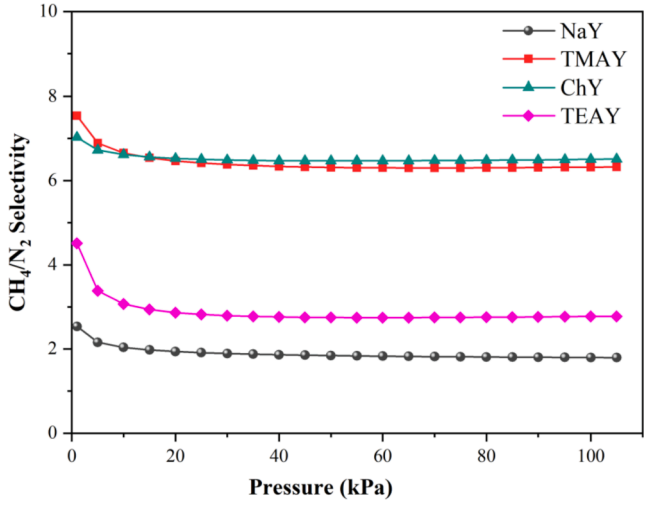

Fig. 9. IAST-predicted selectivities for equimolar CH_4/N_2 mixtures on NaY, TMAY, ChY and TEAY at 25 °C.

interactions between the adsorbents and adsorbates. CH_4 and N_2 adsorption isotherms measured at different temperatures are presented in Fig. S1. Fig. 12 shows the isosteric heats of CH_4 and N_2 adsorption on NaY, TMAY and ChY. Obviously, the isosteric heats of CH_4 and N_2 adsorption on TMAY and ChY were higher than those of NaY. However, the isosteric heats of CH_4 increased more than the isosteric heats of N_2, indicating that ion-exchange with TMA^+ and Ch^+ makes the adsorption affinity of CH_4 to Y zeolite become stronger than that of N_2. The results were also consistent with the previous simulation results. With stronger affinity towards CH_4, TMAY and ChY exhibited increasing CH_4 adsorption amounts despite the decreased S_{BET}. While with relatively weaker affinity towards N_2, N_2 adsorption capacities were predominantly affected by the dramatically decreased S_{BET} and thus N_2 adsorption amounts of TMAY and ChY decreased.

Table 3
CH_4/N_2 selectivities of reported adsorbents at 100 kPa.

Adsorbent	Temperature /°C	CH_4/N_2 selectivity	Reference
TMAY	25	6.32	This work
ChY	25	6.5	This work
PCFT-7	0	6	[15]
$Cu(hfipbb)(H_2hfipbb)_{0.5}$	25	6.9	[14]
$[Ni_3(HCOO)_6]$	25	6.18	[33]
Basolite® A100	25	3.4–4.4	[12]
$^3_\infty$[Cu(Me-4py-trz-ia)]	25	4.0–4.4	[12]
ZIF-68	25	3–4	[34]
MOF-177	25	4.0	[6]
Zeolite 5A	25	0.94	[6]
SAPO-34	25	2.4–3.0	[35]
13X	25	2.36	[8]
Chabazite	0	1.5	[17]
Linde 4A zeolite	0	2.4	[17]
H^+ mordenite	0	2.8	[17]
Mesoporous carbon	25	5.8	[9]
ZnY-pIM	25	7.56	[20]
ZnZSM-5-pIM	25	8.44	[20]

3.6. Breakthrough experiments

To investigate the dynamic separation performances of the adsorbents, breakthrough experiments were carried out with CH_4/N_2 (50:50, v/v) mixtures at 25 °C and 100 kPa. Breakthrough curves of CH_4/N_2 mixtures on NaY, TMAY and ChY are presented in Fig. 13. For all the adsorbents, N_2 firstly broke through the packed bed whereas CH_4 eluted slowly and then reached equilibrium. Notably, the N_2 breakthrough of both TMAY and ChY were much earlier than that of NaY while the CH_4 breakthrough of TMAY and ChY were greatly prolonged compared to NaY. In particular, CH_4 broke through the packed bed in nearly 370 s for TMAY. The breakthrough results confirmed that with the ion-exchange with TMA^+ and Ch^+, CH_4/N_2 separation performances of zeolite Y were

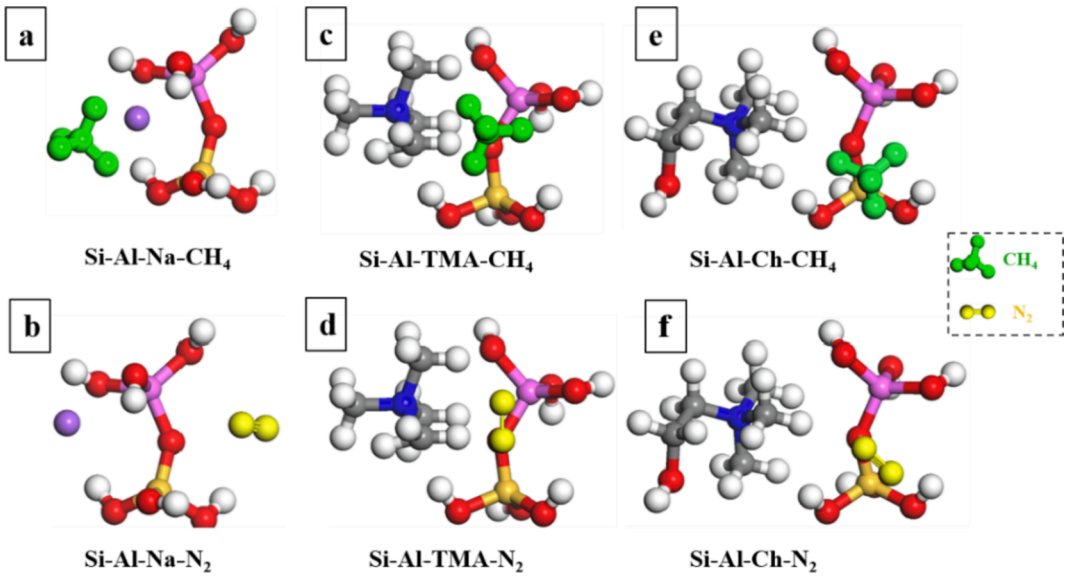

Fig. 10. Lowest energy frameworks of CH_4 and N_2 adsorption in Na^+-Si(1)Al(1) clusters, TMA^+-Si(1)Al(1) clusters and Ch^+-Si(1)Al(1) clusters (white: H, red: O, yellow: Si, lavender: Al, purple: Na, blue: N, gray: C). (For interpretation of the references to colour in this figure legend, the reader is referred to the web version of this article.)

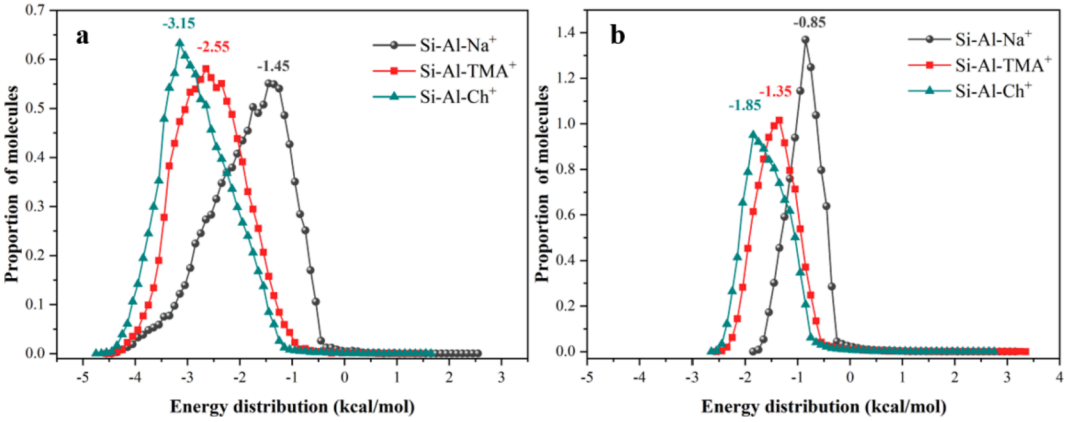

Fig. 11. Energy distribution of (a) CH_4 and (b) N_2 during adsorption in Si(1)Al(1) clusters.

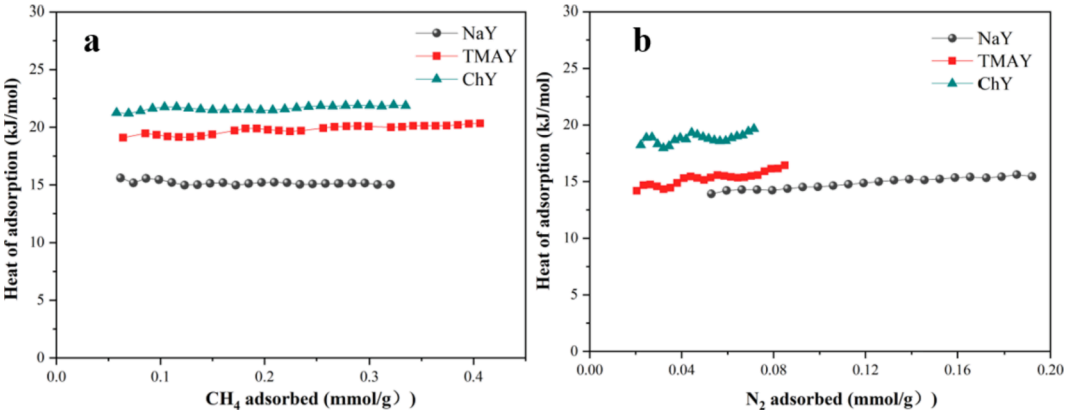

Fig. 12. Isosteric heats of (a) CH_4 and (b) N_2 adsorption on NaY, TMAY and ChY.

significantly improved. The long breakthrough interval between CH_4 and N_2 indicated that TMAY and ChY are highly effective for CH_4/N_2 separation. To investigate the regenerability of the adsorbents, breakthrough cycle experiments were further performed on TMAY at 25 °C and 100 kPa. After each breakthrough experiment, the adsorbent was regenerated in situ at He flow (20 mL/min) at 25 °C for 30 min. As shown in Fig. 14, the breakthrough curves for CH_4/N_2 (50/50) mixtures were almost unchanged with no noticeable decreases in the mean

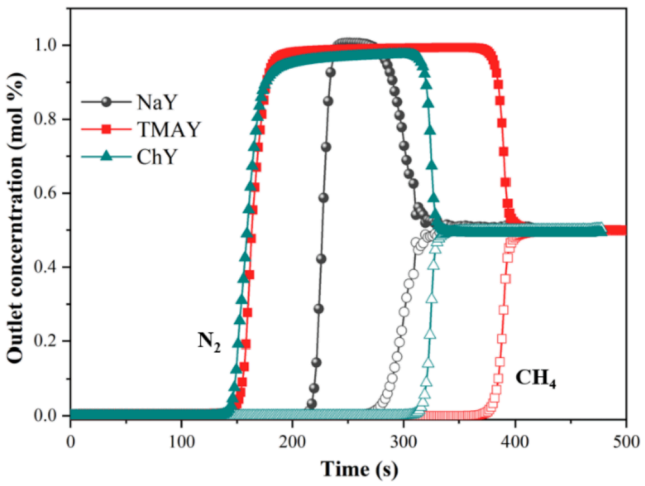

Fig. 13. Breakthrough curves of equimolar CH_4/N_2 (50/50) on NaY, TMAY and ChY at 100 kPa and 25 °C (solid symbols: N_2, open symbols: CH_4).

residence time for both CH_4 and N_2 within the three continuous cycles under 25 °C, revealing that the good regenerability and stability of the adsorbent.

4. Conclusion

In summary, amine cations were introduced into zeolite Y by simple ion-exchange, making the ineffectual zeolite NaY exhibited highly efficient CH_4/N_2 separation performances. With the introduction of large TMA^+ and Ch^+, S_{BET} of resulting samples TMAY and ChY decreased obviously whereas their CH_4 adsorption amounts increased compared to pristine NaY. This is due to the introduction of TMA^+ and Ch^+ resulted in greater interaction affinity of CH_4 with the zeolite framework, which is also verified by the molecular simulations and isosteric heats of adsorption results. TMAY and ChY exhibited relatively high CH_4/N_2 selectivities of 6.32 and 6.50, respectively, at 25 °C and 100 kPa. Breakthrough experiments further confirmed the great CH_4/N_2 separation performances of TMAY and ChY. The efficent separation performances of TMAY and ChY make them promising and applicable adsorbents for CH_4/N_2 separation.

Declaration of Competing Interest

The authors declare that they have no known competing financial interests or personal relationships that could have appeared to influence the work reported in this paper.

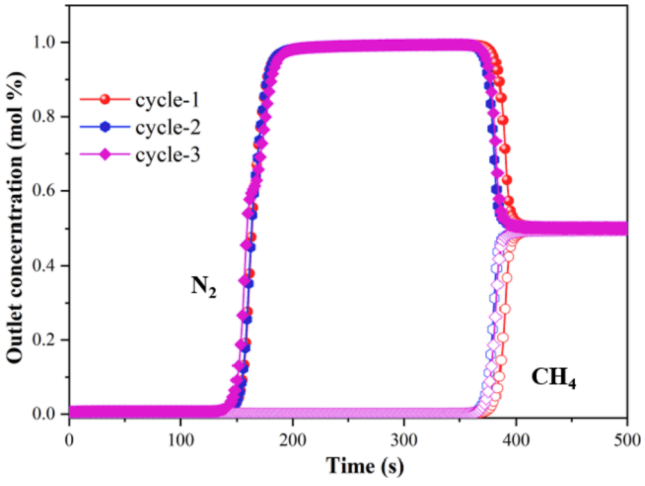

Fig. 14. Breakthrough cycle experiments of equimolar CH_4/N_2 on TMAY at 100 kPa and 25 °C (solid symbols: N_2, open symbols: CH_4).

Acknowledgment

The work was supported by the National Natural Science Foundation of China (Grant No. 21802136).

Appendix A. Supplementary data

Supplementary data to this article can be found online at https://doi.org/10.1016/j.fuel.2021.121077.

References

[1] Tagliabue M, Farrusseng D, Valencia S, Aguado S, Ravon U, Rizzo C, et al. Natural gas treating by selective adsorption: Material science and chemical engineering interplay. Chem Eng J 2009;155(3):553–66.
[2] Zhong D, Englezos P. Methane Separation from Coal Mine Methane Gas by Tetra-n-butyl Ammonium Bromide Semiclathrate Hydrate Formation. Energy Fuels 2012;26(4):2098–106.
[3] Jayaraman A, Hernandez-Maldonado AJ, Yang RT, Chinn D, Munson CL, Mohr DH. Clinoptilolites for nitrogen/methane separation. Chem Eng Sci 2004;59(12):2407–17.
[4] Yu M, Primera-Pedrozo JN, Marcano-González ME, Hernández-Maldonado AJ. Selective adsorption of N2 over CH4 in flexible Sr2+- and Ba2+-UPRM-5 (TEA) titanium silicates: Effect of activation temperature. Chem Eng J 2014;252:311–9.
[5] Yang J, Li J, Wang W, Li L, Li J. Adsorption of CO2, CH4, and N2 on 8-, 10-, and 12-Membered Ring Hydrophobic Microporous High-Silica Zeolites: DDR, Silicalite-1, and Beta. Ind Eng Chem Res 2013;52(50):17856–64.
[6] Saha D, Bao Z, Jia F, Deng S. Adsorption of CO2, CH4, N2O, and N2 on MOF-5, MOF-177, and Zeolite 5A. Environ Sci Technol 2010;44(5):1820–6.
[7] Habgood HW. The kinetics of molecular sieve action. Sorption of nitrogen–methane mixtures by linde molecular sieve 4A. Can J Chem 1958;36(10):1384-97.
[8] Cavenati S, Grande CA, Rodrigues AE. Adsorption Equilibrium of Methane, Carbon Dioxide, and Nitrogen on Zeolite 13X at High Pressures. J Chem Eng Data 2004;49(4):1095–101.
[9] Yuan B, Wu X, Chen Y, Huang J, Luo H, Deng S. Adsorptive separation studies of ethane–methane and methane–nitrogen systems using mesoporous carbon. J Colloid Interface Sci 2013;394:445–50.
[10] Bhadra SJ, Farooq S. Separation of Methane-Nitrogen Mixture by Pressure Swing Adsorption for Natural Gas Upgrading. Ind Eng Chem Res 2011;50(24):14030–45.
[11] Dreisbach F, Staudt R, Keller JU. High pressure adsorption data of methane, nitrogen, carbon dioxide and their binary and ternary mixtures on activated carbon. Adsorption 1999;5(3):215–27.
[12] Möllmer J, Lange M, Möller A, Patzschke C, Stein K, Lässig D, et al. Pure and mixed gas adsorption of CH4 and N2 on the metal–organic framework Basolite® A100 and a novel copper-based 1,2,4-triazolyl isophthalate MOF. J Mater Chem 2012;22(20):10274–86.
[13] Liu B, Smit B. Molecular Simulation Studies of Separation of CO2/N2, CO2/CH4, and CH4/N2 by ZIFs. J Phys Chem C 2010;114(18):8515–22.
[14] Wu X, Yuan B, Bao Z, Deng S. Adsorption of carbon dioxide, methane and nitrogen on an ultramicroporous copper metal–organic framework. J Colloid Interface Sci 2014;430:78–84.
[15] Bhunia A, Boldog I, Möller A, Janiak C. Highly stable nanoporous covalent triazine-based frameworks with an adamantane core for carbon dioxide sorption and separation. J Mater Chem A 2013;1(47):14990–9.
[16] Sircar S. Basic Research Needs for Design of Adsorptive Gas Separation Processes. Ind Eng Chem Res 2006;45(16):5435–48.
[17] Jensen NK, Rufford TE, Watson G, Zhang DK, Chan KI, May EF. Screening Zeolites for Gas Separation Applications Involving Methane, Nitrogen, and Carbon Dioxide. J Chem Eng Data 2012;57(1):106–13.
[18] Harlick PJE, Tezel FH. Adsorption of carbon dioxide, methane, and nitrogen: pure and binary mixture adsorption by ZSM-5 with SiO2/Al2O3 ratio of 30. Sep Sci Technol 2002;37(1):33–60.
[19] Harlick PJE, Tezel FH. Adsorption of carbon dioxide, methane and nitrogen: pure and binary mixture adsorption for ZSM-5 with SiO2/Al2O3 ratio of 280. Sep Purif Technol 2003;33(2):199–210.
[20] Wu Y, Yuan D, He D, Xing J, Zeng S, Xu S, et al. Decorated Traditional Zeolites with Subunits of Metal-Organic Frameworks for CH4/N2 Separation. Angew Chem Int Ed 2019;58(30):10241–4.
[21] Lv D, Shi R, Chen Y, Wu Y, Wu H, Xi H, et al. Selective Adsorption of Ethane over Ethylene in PCN-245: Impacts of Interpenetrated Adsorbent. ACS Appl Mater Interfaces 2018;10(9):8366–73.
[22] Myers AL, Prausnitz JM. Thermodynamics of mixed-gas adsorption. AlChE J 1965;11(1):121–7.
[23] Li B, Zhang Y, Krishna R, Yao K, Han Y, Wu Z, et al. Introduction of π-Complexation into Porous Aromatic Framework for Highly Selective Adsorption of Ethylene over Ethane. J Am Chem Soc 2014;136(24):8654–60.

[24] Kuwahara Y, Nishizawa K, Nakajima T, Kamegawa T, Mori K, Yamashita H. Enhanced Catalytic Activity on Titanosilicate Molecular Sieves Controlled by Cation−π Interactions. J Am Chem Soc 2011;133(32):12462–5.
[25] Yamashita H, Takada S, Hada M, Nakatsuji H, Anpo M. Experimental study and ab initio molecular orbital calculation on the photolysis of n-butyrophenone included within the alkali metal cation-exchanged ZSM-5 zeolite. J Photochem Photobiol A 2003;160(1):37–42.
[26] Rappe AK, Casewit CJ, Colwell KS, Goddard WA, Skiff WM. UFF, a full periodic table force field for molecular mechanics and molecular dynamics simulations. J Am Chem Soc 1992;114(25):10024–35.
[27] Metropolis N, Rosenbluth AW, Rosenbluth MN, Teller AH, Teller E. Equation of State Calculations by Fast Computing Machines. J Chem Phys 1953;21(6):1087–92.
[28] Wang C-C, Juang L-C, Lee C-K, Hsu T-C, Lee J-F, Chao H-P. Effects of exchanged surfactant cations on the pore structure and adsorption characteristics of montmorillonite. J Colloid Interface Sci 2004;280(1):27–35.
[29] Andrade AL, Fabris JD, Ardisson JD, Valente MA, Ferreira JMF. Effect of Tetramethylammonium Hydroxide on Nucleation, Surface Modification and Growth of Magnetic Nanoparticles. J Nanomater 2012;2012:10.
[30] Hunger M, Schenk U, Buchholz A. Mobility of Cations and Guest Compounds in Cesium-Exchanged and Impregnated Zeolites Y and X Investigated by High-Temperature MAS NMR Spectroscopy. J Phys Chem B 2000;104(51):12230–6.
[31] Hayashi S, Suzuki K, Shin S, Hayamizu K, Yamamoto O. High-resolution solid-state 13C NMR spectra of tetramethylammonium ions trapped in zeolites. Chem Phys Lett 1985;113(4):368–71.
[32] Wang Y, Peh SB, Zhao D. Alternatives to Cryogenic Distillation: Advanced Porous Materials in Adsorptive Light Olefin/Paraffin Separations. Small 2019;15(25):1900058.
[33] Guo Y, Hu J, Liu X, Sun T, Zhao S, Wang S. Scalable solvent-free preparation of [Ni3(HCOO)6] frameworks for highly efficient separation of CH4 from N2. Chem Eng J 2017;327:564–72.
[34] Wu H, Zhou W, Yildirim T. Methane Sorption in Nanoporous Metal−Organic Frameworks and First-Order Phase Transition of Confined Methane. J Phys Chem C 2009;113(7):3029–35.
[35] Ren X, Sun T, Hu J, Wang S. Highly enhanced selectivity for the separation of CH4 over N2 on two ultra-microporous frameworks with multiple coordination modes. Microporous Mesoporous Mater 2014;186:137–45.